PHYSICAL REVIEW D **95,** 055025 (2017)

Revisiting $Zb\bar{b}$ couplings in the littlest Higgs model with T parity under current experimental constraints

Bingfang Yang[1,*] and Jinzhong Han[2,†]

[1]*College of Physics and Materials Science, Henan Normal University, Xinxiang 453007, China*
[2]*School of Physics and Telecommunications Engineering, Zhoukou Normal University, Henan 466001, China*

(Received 13 December 2016; published 28 March 2017)

In the littlest Higgs model with T parity (LHT), we revisited $Zb\bar{b}$ couplings under current experimental constraints including the LHC Higgs data and the precision electroweak data. We study the LHT effects in the branching ratio R_b, the forward-backward asymmetry A_{FB}^b and the left- and right-handed couplings g_{Lb}, g_{Rb}. We find that the LHT effects in R_b are sizable enough to be observed at future Z-factories (ILC, CEPC, FCC-ee) in the allowed parameter space, while these effects in A_{FB}^b are weak so that it is difficult to detect at the future experiments. The LHT model provides the large correction to the left-handed coupling g_{Lb}, which can be limited by current and future experiments.

DOI: 10.1103/PhysRevD.95.055025

I. INTRODUCTION

The discovery of the Higgs boson at the Large Hadron Collider (LHC) [1] is a great triumph both in theory and experiment. After this discovery, hunting for new physics (NP) beyond the Standard Model (SM) will be the primary task of the LHC at higher energies. Meanwhile, precision measurements of electroweak physics at future e^+e^- colliders will also offer powerful probes of NP.

Several compelling plans on the next lepton colliders exist, including the International Linear Collider (ILC) [2], the Circular Electron-Position Collider (CEPC) [3] and the Future Circular Collider (FCC-ee)[4]. Such e^+e^- colliders could collect a large amount of data around the Z-pole, producing several orders of magnitude more Z-bosons than what was produced at LEP, so they also are referred to as Z-factories. The large amount of Z-pole data would greatly improve the measurement of the several electroweak precision observables (EWPOs), which could provide strong constraints on NP.

The NP corrections to the $Zb\bar{b}$ couplings are particularly interesting, and many relevant researches have been performed [5,6]. At LEP, the left- and right-handed $Zb\bar{b}$ couplings are mainly determined at the Z-pole by two measurements: the ratio of the $Z \to b\bar{b}$ partial width to the inclusive hadronic width, R_b, and the forward-backward asymmetry of the bottom quark, A_{FB}^b. As an extension of the SM, the littlest Higgs model with T parity (LHT) is one of the popular candidates that can successfully solve the hierarchy problem. The LHT model predicts many new particles, such as heavy gauge bosons, mirror fermions, heavy scalars and heavy top partners. Among them, the top partner usually produces a large correction to the R_b and A_{FB}^b. Moreover, due to the presence of the mirror fermions and their weak interactions with the ordinary fermions, the flavor structure of the LHT model is richer than the one of the SM.

The LHT effects in $Zb\bar{b}$ couplings, especially in R_b, have been studied in the previous works [7] when the Higgs boson was not discovered at the LHC. In this work, we revisit this topic mainly for two reasons: (i) The current experiments, especially the LHC experiments, have severely restrained the LHT parameter space; (ii) given the possibility of some future Z-factories like ILC, CEPC or FCC-ee, a more precise measurement of $Zb\bar{b}$ couplings will help probe the LHT effects. The paper is organized as follows: In Sec. II we give a brief review of the LHT model. In Sec. III we scan over the LHT parameter space and display the LHT effects in R_b^0, A_{FB}^b and the left- and right-handed $Zb\bar{b}$ couplings under current constraints. Finally, we draw our conclusions in Sec. IV.

II. A BRIEF REVIEW OF THE LHT MODEL

The LHT model is based on an $SU(5)/SO(5)$ nonlinear σ model [8], where the $SU(5)$ global symmetry is broken down to $SO(5)$ at the scale $f \sim \mathcal{O}$ (TeV) by the vacuum expectation value (VEV) of the σ field. The VEV also breaks the gauged subgroup $[SU(2) \times U(1)]^2$ of the $SU(5)$ down to the SM electroweak $SU(2)_L \times U(1)_Y$.

After the electroweak symmetry breaking (EWSB), the new T-odd gauge bosons $W_H^{\pm}, Z_H, A_H$ eat the Goldstone bosons $\omega^{\pm}, \omega^0, \eta$ and acquire masses, given at $\mathcal{O}(v^2/f^2)$ by

$$M_{W_H} = M_{Z_H} = gf\left(1 - \frac{v^2}{8f^2}\right), \quad M_{A_H} = \frac{g'f}{\sqrt{5}}\left(1 - \frac{5v^2}{8f^2}\right), \tag{1}$$

*yangbingfang@htu.edu.cn
†hanjinzhong@zknu.edu.cn

with g and g' being the SM $SU(2)$ and $U(1)$ gauge couplings, respectively.

The T-even $W^{\pm}$ and Z bosons eat the Goldstone bosons $\pi^{\pm}, \pi^0$ and acquire masses, given at $\mathcal{O}(v^2/f^2)$ by

$$M_W = \frac{gv}{2}\left(1-\frac{v^2}{12f^2}\right), \qquad M_Z = \frac{gv}{2\cos\theta_W}\left(1-\frac{v^2}{12f^2}\right). \tag{2}$$

The photon A is also T-even and remains massless. Here, v represents the Higgs doublet VEV, which can be given by

$$v = \frac{f}{\sqrt{2}}\arccos\left(1-\frac{v_{\rm SM}^2}{f^2}\right) \simeq v_{\rm SM}\left(1+\frac{1}{12}\frac{v_{\rm SM}^2}{f^2}\right), \tag{3}$$

where $v_{\rm SM} = 246$ GeV is the SM Higgs VEV.

To implement T parity in the fermion sector, it requires the introduction of mirror fermions. The T-odd mirror partners for each SM fermion are added and a Yukawa-type interaction can be written down to give them masses

$$\mathcal{L}_{\rm mirror} = -\kappa_{ij} f(\bar{\Psi}_2^i \xi + \bar{\Psi}_1^i \Sigma_0 \Omega \xi^{\dagger}\Omega)\Psi_R^j + \text{H.c.}, \tag{4}$$

where $i, j = 1, 2, 3$ are the generation indices. After EWSB, the mirror fermions acquire masses, given at $\mathcal{O}(v^2/f^2)$ by

$$m_{d_H^i} = \sqrt{2}\kappa_i f, \qquad m_{u_H^i} = m_{d_H^i}\left(1-\frac{v^2}{8f^2}\right), \tag{5}$$

$$m_{l_H^i} = \sqrt{2}\kappa_i f, \qquad m_{\nu_H^i} = m_{l_H^i}\left(1-\frac{v^2}{8f^2}\right), \tag{6}$$

where κ_i are the eigenvalues of the mass matrix κ.

As discussed in Ref. [9], the existence of four Cabibbo-Kobayashi-Maskawa (CKM)-like unitary mixing matrices V_{Hu}, V_{Hd}, V_{Hl} and $V_{H\nu}$ is one of the important ingredients in the mirror fermion sector. Note that V_{Hu} and V_{Hd} satisfy the physical constraint $V_{Hu}^{\dagger}V_{Hd} = V_{\rm CKM}$ and V_{Hl} and $V_{H\nu}$ satisfy the physical constraint $V_{H\nu}^{\dagger}V_{Hl} = V_{\rm PMNS}^{\dagger}$, where $V_{\rm PMNS}$ is the Pontecorvo-Maki-Nakagata-Saki (PMNS) matrix. We can parametrize V_{Hd} with three angles $\theta_{12}^d, \theta_{23}^d, \theta_{13}^d$ and three phases $\delta_{12}^d, \delta_{23}^d, \delta_{13}^d$ [10]:

$$V_{Hd} = \begin{pmatrix} c_{12}^d c_{13}^d & s_{12}^d c_{13}^d e^{-i\delta_{12}^d} & s_{13}^d e^{-i\delta_{13}^d} \\ -s_{12}^d c_{23}^d e^{i\delta_{12}^d} - c_{12}^d s_{23}^d s_{13}^d e^{i(\delta_{13}^d-\delta_{23}^d)} & c_{12}^d c_{23}^d - s_{12}^d s_{23}^d s_{13}^d e^{i(\delta_{13}^d-\delta_{12}^d-\delta_{23}^d)} & s_{23}^d c_{13}^d e^{-i\delta_{23}^d} \\ s_{12}^d s_{23}^d e^{i(\delta_{12}^d+\delta_{23}^d)} - c_{12}^d c_{23}^d s_{13}^d e^{i\delta_{13}^d} & -c_{12}^d s_{23}^d e^{i\delta_{23}^d} - s_{12}^d c_{23}^d s_{13}^d e^{i(\delta_{13}^d-\delta_{12}^d)} & c_{23}^d c_{13}^d \end{pmatrix}. \tag{7}$$

To stabilize the Higgs mass, an additional T-even top partner T^+ is introduced to cancel the large one-loop quadratic divergences caused by the top quark. Meanwhile, the implementation of T parity requires a T-odd mirror partner T^- with T^+. The T-even quark T^+ mixes with the SM top quark and the mixing can be parametrized by the ratio $R = \lambda_1/\lambda_2$, where λ_1 and λ_2 are two dimensionless top quark Yukawa couplings. Then, the masses of the top quark and its partners are given at $\mathcal{O}(v^2/f^2)$ by

$$\begin{aligned} m_t &= \frac{\lambda_2 vR}{\sqrt{1+R^2}}\left[1+\frac{v^2}{f^2}\left(-\frac{1}{3}+\frac{1}{2}\frac{R^2}{(1+R^2)^2}\right)\right] \\ m_{T^+} &= \frac{f}{v}\frac{m_t(1+R^2)}{R}\left[1+\frac{v^2}{f^2}\left(\frac{1}{3}-\frac{R^2}{(1+R^2)^2}\right)\right)\right] \\ m_{T^-} &= \frac{f}{v}\frac{m_t\sqrt{1+R^2}}{R}\left[1+\frac{v^2}{f^2}\left(\frac{1}{3}-\frac{1}{2}\frac{R^2}{(1+R^2)^2}\right)\right)\right]. \end{aligned} \tag{8}$$

For the down-type quarks and charged leptons, there are usually two possible ways (they are denoted as case A and case B) to construct the Yukawa interactions [11]. At order $\mathcal{O}(v_{\rm SM}^4/f^4)$, the corresponding corrections to the Higgs couplings with respect to their SM values are given by ($d \equiv d, s, b, \ell_i^{\pm}$)

$$\begin{aligned} \frac{g_{h\bar{d}d}}{g_{h\bar{d}d}^{\rm SM}} &= 1-\frac{1}{4}\frac{v_{\rm SM}^2}{f^2}+\frac{7}{32}\frac{v_{\rm SM}^4}{f^4} \quad \text{case A} \\ \frac{g_{h\bar{d}d}}{g_{h\bar{d}d}^{\rm SM}} &= 1-\frac{5}{4}\frac{v_{\rm SM}^2}{f^2}-\frac{17}{32}\frac{v_{\rm SM}^4}{f^4} \quad \text{case B}. \end{aligned} \tag{9}$$

III. NUMERICAL CALCULATIONS AND RESULTS

In the LHT model, the one-loop Feynman diagrams of the mirror quark correction to $Zb\bar{b}$ vertex and the top partner correction to $Zb\bar{b}$ vertex are shown in Figs. 1 and 2, respectively.

To be clear at a glance, we show the Feynman diagrams in the unitary gauge. If the 't Hooft-Feynman gauge is chosen, the contributions of Goldstone bosons $(\omega^{\pm}, \omega^0, \eta, \pi^{\pm})$ should be involved. We can see that the flavor violating interactions between SM quarks and mirror quarks are mediated by the gauge bosons $W^{\pm}, A_H, Z_H, W_H^{\pm}$. Each loop diagram is composed of some scalar loop functions [12], which calculated by using LoopTools [13] straightforwardly.

In our numerical calculations, the SM parameters are taken as follows [14]:

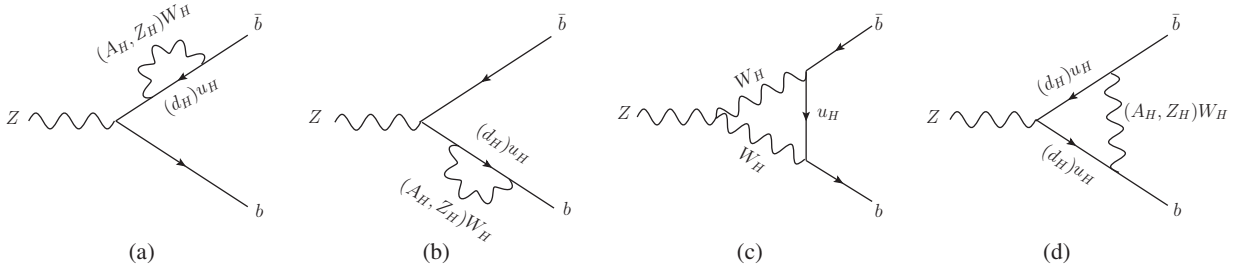

FIG. 1. One-loop Feynman diagrams of the mirror quark correction to $Zb\bar{b}$.

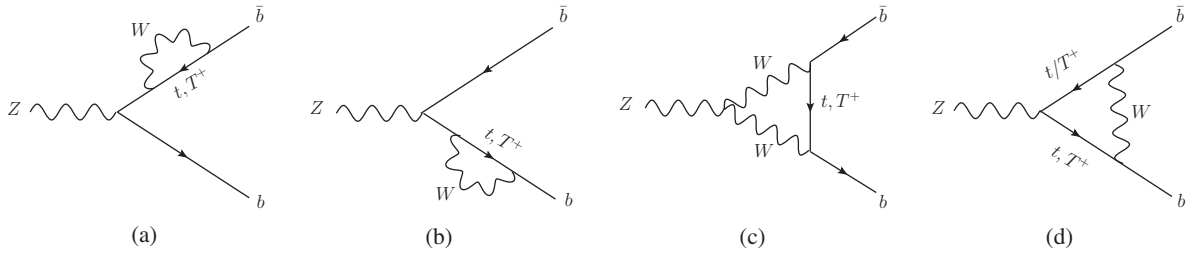

FIG. 2. One-loop Feynman diagrams of the top partner correction to $Zb\bar{b}$.

$$\sin^2\theta_W = 0.231, \quad \alpha_e = 1/128, \quad M_Z = 91.1876\ \text{GeV}, \quad m_h = 125\ \text{GeV}, \quad m_t = 173.21\ \text{GeV}.$$

The LHT parameters related to our calculations are the scale f, the ratio R, the Yukawa couplings κ_i of the mirror fermions and the parameters in the matrices V_{Hu}, V_{Hd}. For the mirror fermion masses, we assume the first two generations are degenerate:

$$m_{u_H^{1,2}} = m_{d_H^{1,2}} = m_{l_H^{1,2}} = m_{\nu_H^{1,2}} = M_{12},$$
$$m_{u_H^3} = m_{d_H^3} = m_{l_H^3} = m_{\nu_H^3} = M_3. \tag{10}$$

Considering the constraint from Ref. [15], we scan over these parameters within the following ranges:

$$500\ \text{GeV} \le f \le 2000\ \text{GeV}, \quad 0.6 \le \kappa_i \le 3, \quad 0.1 \le R \le 3.3,$$

where $\kappa_1 = \kappa_2 \neq \kappa_3$ though they have the same range.

For the parameters in the matrices V_{Hu}, V_{Hd}, we consider two scenarios as follows:

$$\text{Scenario I}: \ V_{Hd} = 1, \quad V_{Hu} = V_{\text{CKM}}^\dagger$$
$$\text{Scenario II}: \ s_{13}^d = 0.5, \quad \delta_{12}^d = \delta_{23}^d = 0, \quad \delta_{13}^d = \delta_{13}^{\text{SM}}, \quad s_{ij}^d = s_{ij}^{\text{SM}}, \quad \text{otherwise}.$$

A. R_b in the LHT

We employ the following notation for the effective $Zb\bar{b}$ interaction:

$$L_{Zb\bar{b}} = \frac{g}{\cos\theta_W} Z_\mu (g_{Lb}\bar{b}_L\gamma^\mu b_L + g_{Rb}\bar{b}_R\gamma^\mu b_R), \tag{11}$$

where θ_W is the Weinberg angle.

We shall use δg_{Lb} and δg_{Rb} to parametrize the corrections of the $Zb\bar{b}$ couplings, defined as

$$g_{Lb} = g_{Lb}^{\text{SM}} + \delta g_{Lb}, \qquad g_{Rb} = g_{Rb}^{\text{SM}} + \delta g_{Rb}, \tag{12}$$

where g_{Lb}^{SM} and g_{Rb}^{SM} are the SM predictions for g_{Lb} and g_{Rb}, $\delta g_{\lambda b}$ $(\lambda = L, R)$ is given by

$$\delta g_{\lambda b} = \Gamma_{f\lambda}(m_Z^2) - g_\lambda^{Zb\bar{b}} \Sigma_{b\lambda}(m_b^2), \tag{13}$$

where $\Gamma_{f\lambda}(m_Z^2)$ denotes the vertex loop contributions and $\Sigma_{b\lambda}(m_b^2)$ is the counterterm from the bottom quark self-energy. In the numerical calculations, we applied the on-shell renormalization scheme to remove the ultraviolet divergences.

The one-loop LHT correction to R_b can be expressed as

$$\delta R_b^{\text{LHT}} \simeq \frac{2R_b^{\text{SM}}(1 - R_b^{\text{SM}})}{g_{Vb}^2(3-\beta^2) + 2g_{Ab}^2\beta^2} \times [g_{Vb}(3-\beta^2)\delta g_{Vb} + 2g_{Ab}\beta^2\delta g_{Ab}], \tag{14}$$

where the SM prediction $R_b^{\text{SM}} = 0.21578 \pm 0.00011$, $g_{Vb} = -1/2 + 2\sin^2\theta_W/3$ and $g_{Ab} = -1/2$ are respectively the vector and axial vector couplings of tree-level $Zb\bar{b}$ interaction, $\beta = \sqrt{1 - 4m_b^2/m_Z^2}$ is the velocity of bottom quark in $Z \to b\bar{b}$, and δg_{Vb}, δg_{Ab} are the corresponding corrections, defined as [16]

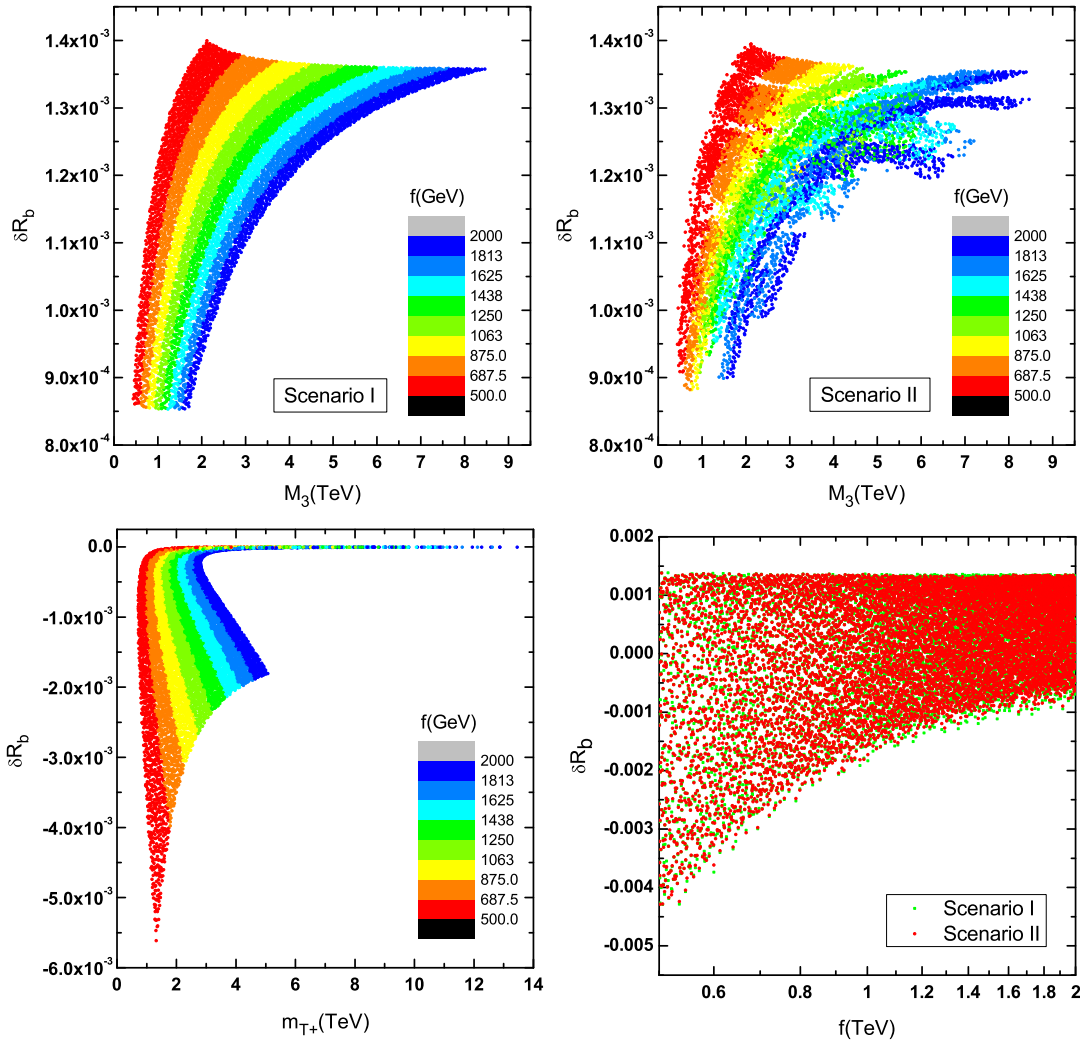

FIG. 3. The scatter plots of the mirror quark one-loop effects (top left and top right), the top partner one-loop effects (bottom left) and the R_b (bottom right) in two scenarios.

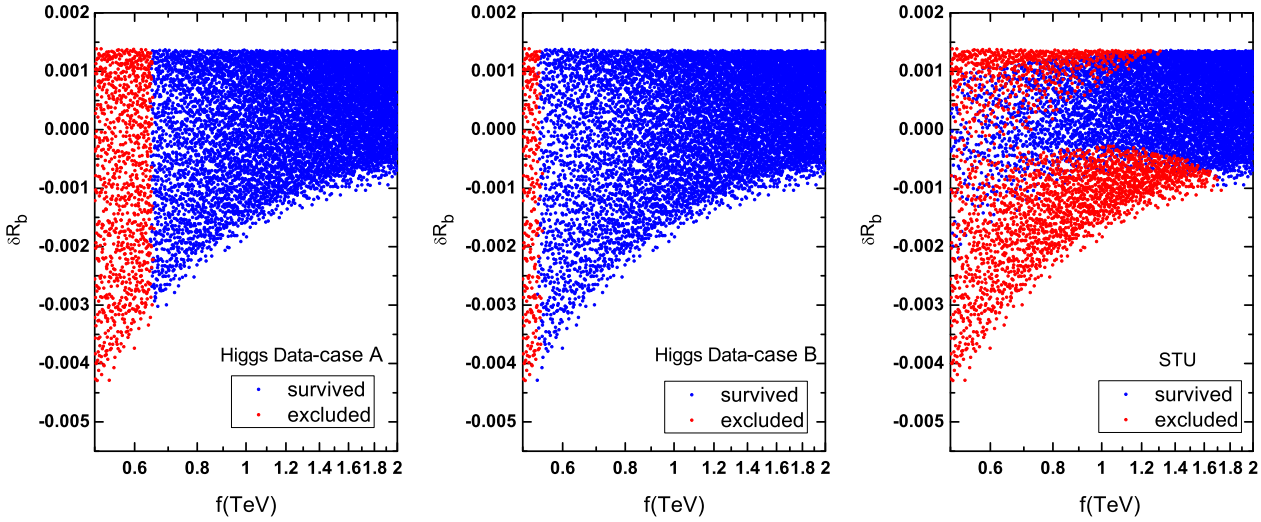

FIG. 4. The plots of survived samples on δR_b, showing the constraint of the Higgs data in two cases and the constraint of the oblique parameters S, T, U, where the samples with and without the relevant constraints at 2σ level are displayed.

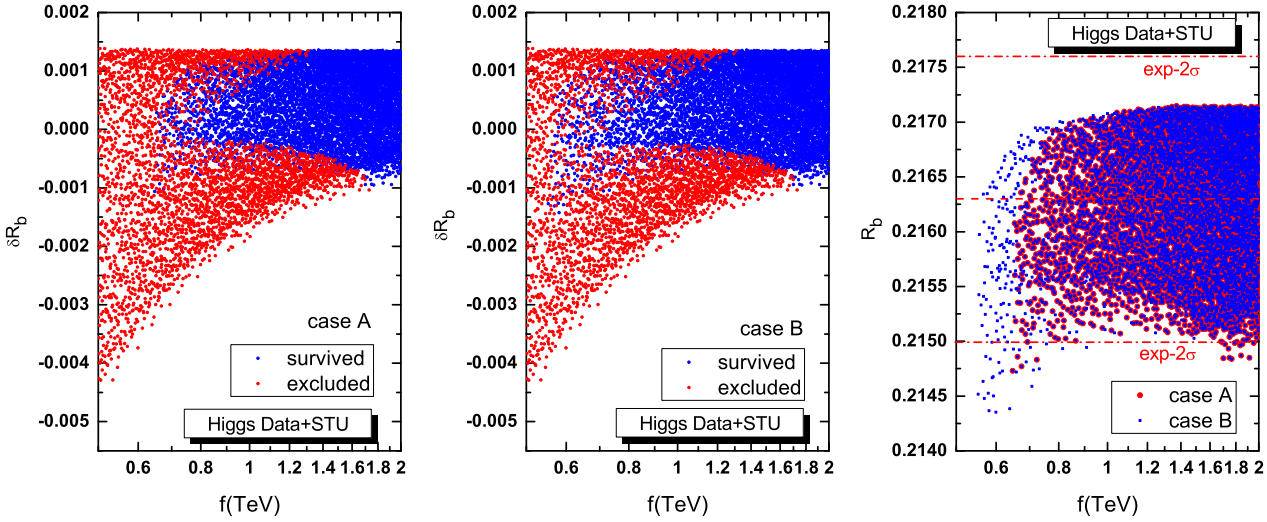

FIG. 5. The plots of survived samples on δR_b, showing the combined constraints of the Higgs data and the oblique parameters S, T, U in two cases, where the samples with and without the combined constraints at the 2σ level are displayed. In the right panel, the survived samples on the R_b are displayed, where the experimental value $R_b^{\rm exp} = 0.21629 \pm 0.00066$.

$$\delta g_{Vb} = \frac{\delta g_{Lb} + \delta g_{Rb}}{2}, \qquad \delta g_{Ab} = \frac{\delta g_{Lb} - \delta g_{Rb}}{2}. \quad (15)$$

In Fig. 3, we show the scatter plots of the mirror quark one-loop effects and the top partner one-loop effects in R_b, which corresponds to the one-loop Feynman diagrams in Figs. 1 and 2, respectively. We can see that the contribution of the mirror quark is positive and the contribution of the top partner is negative, of which the contribution from the top partner is dominant. For scenario I, the matrix V_{Hd} is diagonal so that the first two generation mirror quarks do not contribute to the corrections. For scenario II, this is a large mixing scenario and the first two generation mirror quarks can contribute to the corrections due to the presence of the off-diagonal elements. Comparing scenario I with scenario II, we can see that the samples from the mirror quarks fall in almost the same range though the distributions are somewhat different. It is worth noting that the changes in δR_b for the two scenarios are tiny, which is because the dominant top partner correction is independent of the matrix V_{Hd}. Since the δR_b only has a weak dependence on the V_{Hd} choice, we will take scenario I as an example in the following analysis.

In Fig. 4, we show the plots of survived samples on δR_b under the current Higgs data in two cases and the constraint of the EWPOs. We perform the fit of Higgs data by using HiggsSignals-1.4.0 [17], which includes the available Higgs data sets from the ATLAS, CMS, CDF and D0 collaborations. For constraint of the Higgs data, we can see that the δR_b can respectively reach -0.003 and -0.004 for case A and case B at the 2σ level. The EWPO can be described in terms of the well-known S, T, U oblique parameters [18]. We perform the EWPO fit by using the formulas in Ref. [19] and taking $S = 0.05 \pm 0.10$, $T = 0.08 \pm 0.12$, $U = 0.02 \pm 0.10$ [14]. For constraint of the oblique parameters, we can see that the δR_b can reach -0.002 at the 2σ level. Furthermore, we can see that the constraint of the oblique parameters can exclude more samples than the Higgs data while it restricts the scale f relatively loosely.

In Fig. 5, we show the plots of survived samples on δR_b under the combined constraints of the Higgs data and the oblique parameters S, T, U in two cases, where the samples with and without the combined constraints at the 2σ level are displayed. In order to see the overall situation of R_b, we also show the survived samples on R_b with the combined constraints at the 2σ level in the right panel of Fig. 5. We can see that most of the survived samples fall within the 2σ region of its experimental value, which means that the current R_b measurement restricts the LHT model parameters relaxedly. In Table I, we show the estimated precision reach for the observables most relevant to constrain the $Zb\bar{b}$

TABLE I. The estimated precision reach for the observables most relevant to constrain the $Zb\bar{b}$ coupling at future colliders. In each entry, the number at the top shows the total uncertainty while the number at the bottom (in parentheses) shows the corresponding systematic uncertainty. The last row shows the expected number $\mathcal{N}_Z$ of Z events that will be collected.

	Precision			
Observable	Current	CEPC	ILC	FCC-ee
R_b^0	0.00066	0.00017	0.00014	0.00006
[0.21629]	(0.00050)	(0.00016)		(0.00006)
$A_{FB}^{0,b}$	0.0016	0.00015		
[0.0992]	(0.0007)	(0.00014)		
$\mathcal{N}_Z$	$\sim 2 \times 10^7$	$\sim 2 \times 10^9$	$\sim 10^9$	$\sim 10^{12}$

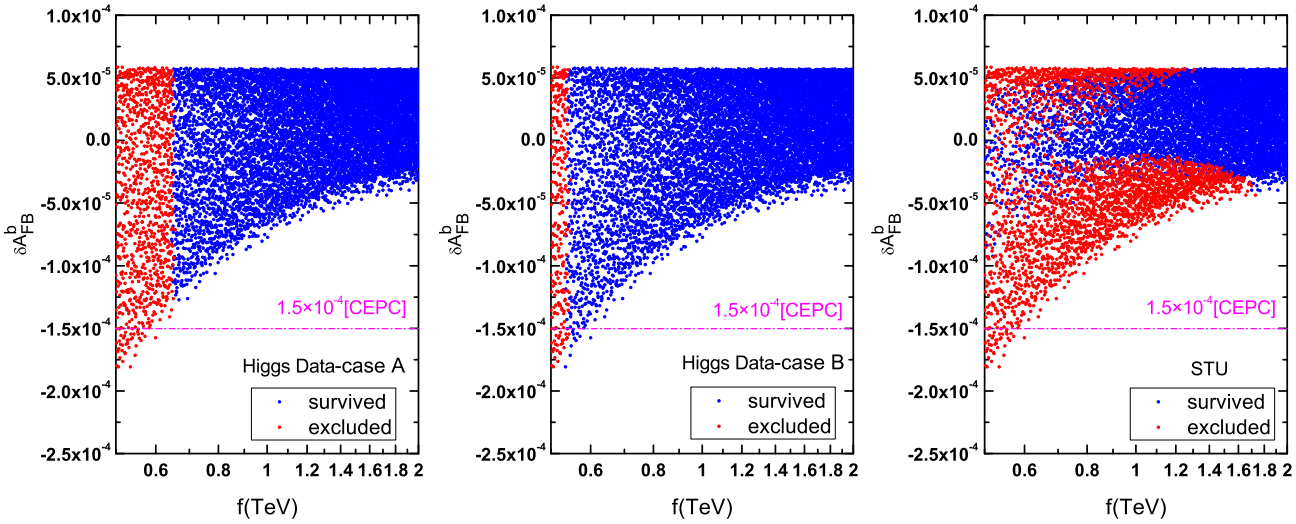

FIG. 6. Same as Fig. 4, but for A_{FB}^{b}.

coupling at future colliders. From Table I, we can see that the future colliders will give more severe constraints to the LHT model parameters.

B. A_{FB}^{b} in the LHT

In addition to R_b, we also show the LHT effects in the forward-backward asymmetry A_{FB}^{b} in the decay $Z \to \bar{b}b$:

$$\delta A_{FB}^{b,\mathrm{LHT}} \simeq A_{FB}^{b,\mathrm{SM}} \left(\frac{g_{Vb}\delta g_{Vb} + g_{Ab}\delta g_{Ab}}{g_{Ab}g_{Vb}} - 2\frac{g_{Vb}(3-\beta^2)\delta g_{Vb} + 2g_{Ab}\beta^2\delta g_{Ab}}{g_{Vb}^2(3-\beta^2) + 2g_{Ab}^2\beta^2} \right), \quad (16)$$

where the SM prediction $A_{FB}^{b,\mathrm{SM}} = 0.1032 \pm 0.0004$.

In Fig. 6, we show the plots of survived samples on δA_{FB}^{b} under the current Higgs data in two cases and the constraint of the oblique parameters S, T, U, where the samples with and without the relevant constraints at the 2σ level are displayed. In Fig. 7, we show the same result as Fig. 6, but for the combined constraints of Higgs data and oblique parameters. We also show the survived samples on A_{FB}^{b} in the right panel of Fig. 7, and can see the plots of A_{FB}^{b} are entirely out of the 2σ region of its experimental value. Recently, the global electroweak fit results using newest next-to-next-to-leading-order theoretical predictions [20] show that the experimental value $A_{FB}^{b,\mathrm{exp}}$ still disagrees with the SM prediction $A_{FB}^{b,\mathrm{SM}}$ by -2.5σ. Some people believe this significant deviation may be a window into the NP. For the LHT model, we can see that it cannot alleviate the tension between experimental measurement and SM

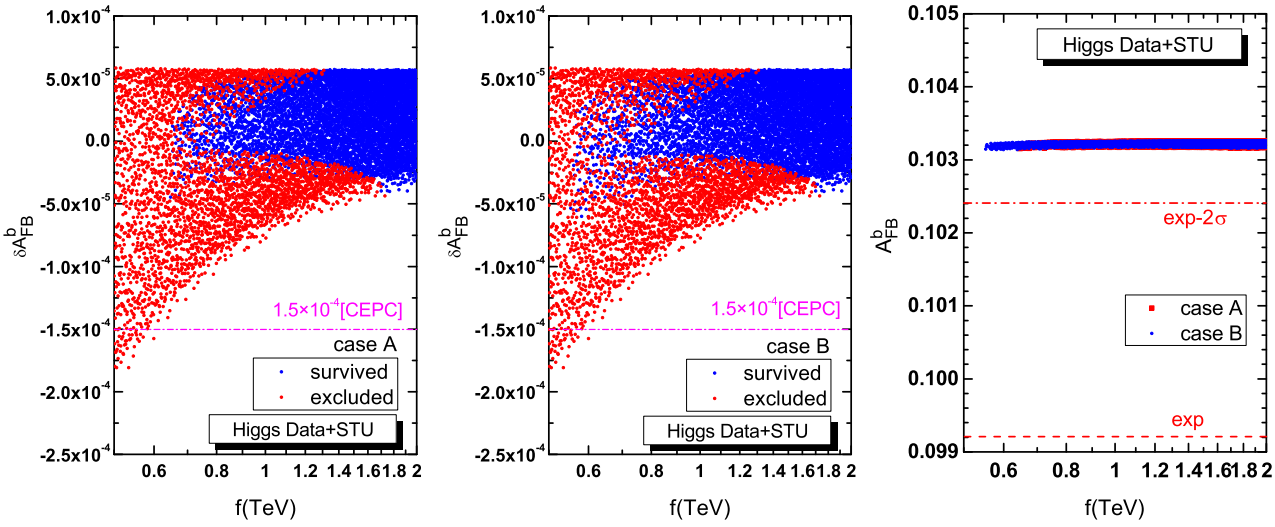

FIG. 7. Same as Fig. 5, but for A_{FB}^{b}, where the experimental value $A_{FB}^{b,\mathrm{exp}} = 0.0992 \pm 0.0016$.

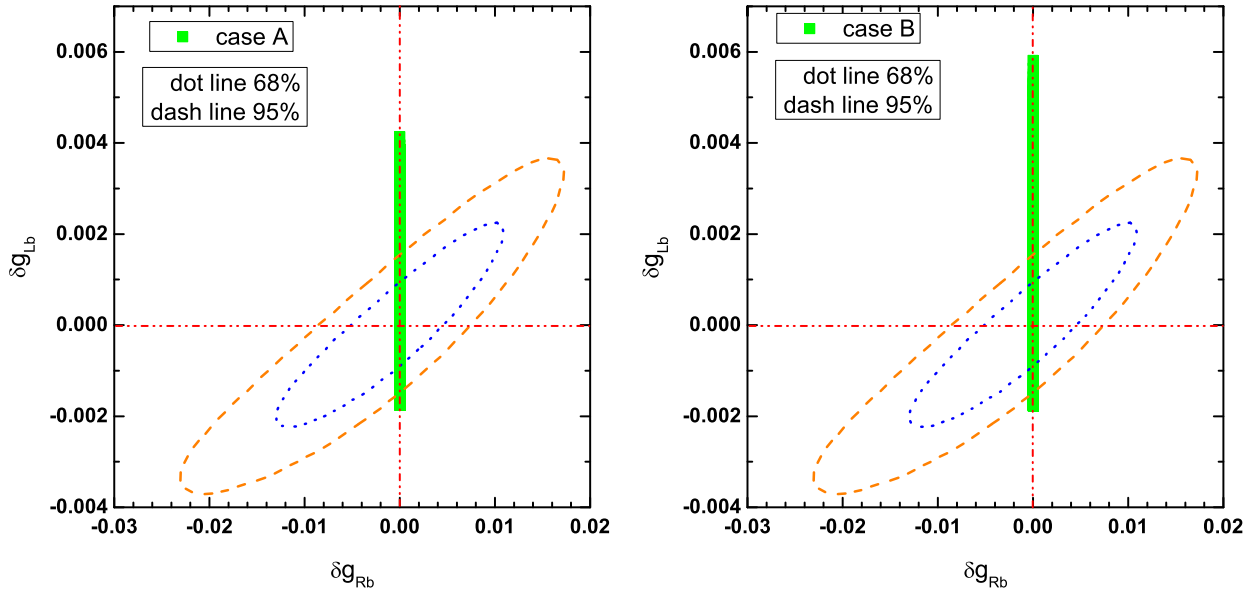

FIG. 8. Preferred regions in the $(\delta g_{Lb},\delta g_{Rb})$ plane for case A (left) and case B (right), assuming SM central values and current precision for all measurements.

prediction of A_{FB}^b substantially since it cannot provide a large correction to the A_{FB}^b.

For the future precision of A_{FB}^b measurement, the CEPC would produce 2×10^9 Z-bosons and probably measure A_{FB}^b with an uncertainty of 1.5×10^{-4}, which is marked on Figs. 6 and 7. Unfortunately, we can see that it is quite difficult to test the LHT effects in A_{FB}^b measurement at the CEPC.

C. g_{Lb} and g_{Rb} in the LHT

In Fig. 8, we show the preferred regions in the $(\delta g_{Lb},\delta g_{Rb})$ plane for case A (left) and case B (right), assuming SM central values for all measurements. We can see that the LHT model gives a sizable correction to the left-handed coupling g_{Lb} while little correction to the right-handed coupling g_{Rb}. The dotted and dashed lines of the contours are respectively 68% C.L. and 95% C.L. corresponding to the current precision, which has been obtained by global fit in Ref. [6].

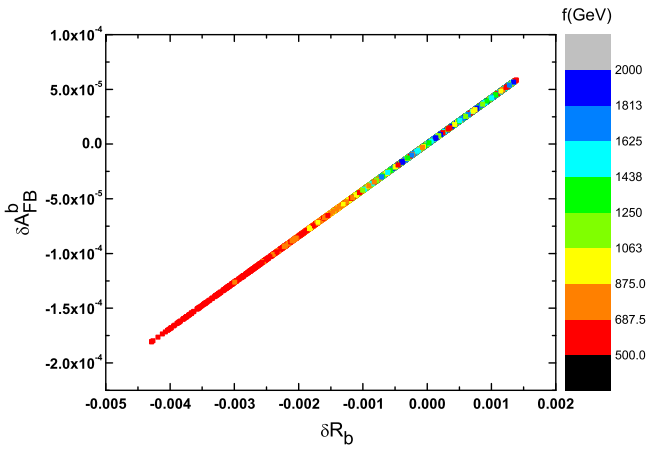

FIG. 9. Correlation between δR_b and δA_{FB}^b.

D. Correlation between δR_b and δA_{FB}^b

In Fig. 9, we show the correlation between δR_b and δA_{FB}^b, where the combined constraints of Higgs data and EWPO are not be taken into account. From Fig. 9 we can see that δR_b and δA_{FB}^b are strongly correlated. Actually, both δR_b and δA_{FB}^b are the linear combinations of the left-handed correction δg_{Lb} and right-handed correction δg_{Rb}, combined with $\delta g_{Lb} \gg \delta g_{Rb}$ as shown in Fig. 8, so that δR_b and δA_{FB}^b must be almost proportional to each other.

IV. CONCLUSIONS

In this paper, we revisited the LHT effects in $Zb\bar{b}$ couplings under current experimental constraints including the LHC Higgs data and the EWPOs. We scanned over the LHT parameter space and displayed the LHT effects in R_b, A_{FB}^b and couplings g_{Lb}, g_{Rb}. We found that the LHT effects can alter R_b with a magnitude sizable enough to be observed at future Z-factories (ILC, CEPC, FCC-ee) although the LHT parameter space has been severely restrained by current experimental data. The LHT effects in A_{FB}^b are weak under current experimental constraints so that this effect is difficult to detect at the future CEPC. The LHT correction to $Zb\bar{b}$ couplings focuses on the left-handed coupling g_{Lb}, which will be restricted by current and future measurements.

ACKNOWLEDGMENTS

This work is supported by the National Natural Science Foundation of China (NNSFC) under Grants No. U1404113 and No. 11405047, and by the Startup Foundation for Doctors of Henan Normal University under Grant No. qd15207, the Aid Project for the Mainstay Young Teachers in Henan Provincial Institutions of Higher Education (2016GGJS-135).

[1] G. Aad *et al.* (ATLAS Collaboration), Phys. Lett. B **710**, 49 (2012); S. Chatrachyan *et al.* (CMS Collaboration), Phys. Lett. B **710**, 26 (2012).
[2] H. Baer, T. Barklow, K. Fujii, Y. Gao, A. Hoang *et al.*, arXiv:1306.6352.
[3] M. Ahmad *et al.*, CEPC-SPPC preliminary conceptual design report, Volume I: Physics and detector, http://cepc.ihep.ac.cn/preCDR/volume.html, 2015.
[4] M. Bicer *et al.* (TLEP Design Study Working Group Collaboration), J. High Energy Phys. 01 (2014) 164.
[5] See examples: H. E. Haber and H. E. Logan, Phys. Rev. D **62**, 015011 (2000); K. Agashe, R. Contino, L. Da Rold, and A. Pomarol, Phys. Lett. B **641**, 62 (2006); J. Cao and J. M. Yang, J. High Energy Phys. 12 (2008) 006; G. Bhattacharyya, A. Kundu, and T. S. Ray, J. Phys. G **41**, 035002 (2014); D. Choudhury, A. Kundu, and P. Saha, Phys. Rev. D **89**, 013002 (2014); W. Su and J. M. Yang, Phys. Lett. B **757**, 136 (2016).
[6] S. Gori, J. Y. Gu, and L.-T. Wang, J. High Energy Phys. 04 (2016) 062.
[7] X.-F. Han, Phys. Rev. D **80**, 055027 (2009); B. F. Yang, X. L. Wang, and J. Z. Han, Nucl. Phys. **B847**, 1 (2011).
[8] H. C. Cheng and I. Low, J. High Energy Phys. 09 (2003) 051; 08 (2004) 061; I. Low, J. High Energy Phys. 10 (2004) 067; J. Hubisz and P. Meade, Phys. Rev. D **71**, 035016 (2005).
[9] J. Hubisz, S. J. Lee, and G. Paz, J. High Energy Phys. 06 (2006) 041.
[10] M. Blanke, A. J. Buras, A. Poschenrieder, S. Recksiegel, C. Tarantino, S. Uhlig, and A. Weiler, Phys. Lett. B **646**, 253 (2007).
[11] C. R. Chen, K. Tobe, and C. P. Yuan, Phys. Lett. B **640**, 263 (2006).
[12] G. 't Hooft and M. J. G. Veltman, Nucl. Phys. **B153**, 365 (1979).
[13] T. Hahn and M. Perez-Victoria, Comput. Phys. Commun. **118**, 153 (1999); T. Hahn, Nucl. Phys. B, Proc. Suppl. **135**, 333 (2004).
[14] C. Patrignani and K. A. Olive(Particle Data Group), Chin. Phys. C **40**, 100001 (2016).
[15] J. Hubisz, P. Meade, A. Noble, and M. Perelstein, J. High Energy Phys. 01 (2006) 135; A. Belyaev, C. R. Chen, K. Tobe, and C. P. Yuan, Phys. Rev. D **74**, 115020 (2006); Q. H. Cao and C. R. Chen, Phys. Rev. D **76**, 075007 (2007); J. Reuter and M. Tonini, J. High Energy Phys. 02 (2013) 077; J. Reuter, M. Tonini, and M. de Vries, J. High Energy Phys. 02 (2014) 053; B. F. Yang, G. F. Mi, and N. Liu, J. High Energy Phys. 10 (2014) 047; N. Liu, L. Wu, B. F. Yang, and M. C. Zhang, Phys. Lett. B **753**, 664 (2016); B. F. Yang, J. Z. Han, and N. Liu, Phys. Rev. D **95**, 035010 (2017).
[16] M. Bohm, H. Spiesberger, and W. Hollik, Fortschr. Phys. **34**, 687 (1986); W. F. L. Hollik, Fortschr. Phys. **38**, 165 (1990).
[17] P. Bechtle, S. Heinemeyer, O. Stål, T. Stefaniak, and G. Weiglein, Eur. Phys. J. C **74**, 2711 (2014); Comput. Phys. Commun. **181**, 138 (2010).
[18] M. E. Peskin and T. Takeuchi, Phys. Rev. D **46**, 381 (1992).
[19] J. Hubisz, P. Meade, A. Noble, and M. Perelstein, J. High Energy Phys. 01 (2006) 135.
[20] M. Baak, J. Cúth, J. Haller, A. Hoecker, R. Kogler, K. Mönig, M. Schott, and J. Stelzer (Gfitter Group Collaboration), Eur. Phys. J. C **74**, 3046 (2014).